Research Paper
J. Astron. Space Sci. 31(4), 295-301 (2014)
http://dx.doi.org/10.5140/JASS.2014.31.4.295

JASS Journal of Astronomy and Space Sciences

A Statistical Test of the Relationship Between Chorus Wave Activation and Anisotropy of Electron Phase Space Density

Dong-Hee Lee, Dae-Young Lee†, Dae-Kyu Shin, Jin-Hee Kim, Jung-Hee Cho
Department of Astronomy and Space Science, Chungbuk National University, Cheongju 361-763, Korea

Whistler mode chorus wave is considered to play a critical role in accelerating and precipitating the electrons in the outer radiation belt. In this paper we test a conventional scenario of triggering chorus using THEMIS satellite observations of waves and particles. Specifically, we test if the chorus onset is consistent with development of anisotropy in the electron phase space density (PSD). After analyzing electron PSD for 73 chorus events, we find that, for ~80 % of them, their onsets are indeed associated with development of the positive anisotropy in PSD where the pitch angle distribution of electron velocity peaks at 90 degrees. This PSD anisotropy is prominent mainly at the electron energy range of ≤ ~20 keV. Interestingly, we further find that there is sometimes a time delay among energies in the increases of the anisotropy: A development of the positive anisotropy occurs earlier by several minutes for lower energy than for an adjacent higher energy.

Keywords: whistler chorus, radiation belt electrons, wave-particle interaction

1. INTRODUCTION

Plasma waves of various kinds exist within the Earth's magnetosphere, playing a critical role in accelerating, scattering, and redistributing plasma particles. In particular, the inner magnetosphere that contains the radiation belts and the ring current is often full of plasma waves at various frequency ranges such as electron cyclotron waves, whistler mode waves, electromagnetic ion cyclotron waves, MHD waves. Some of these waves can strongly interact with or be generated by electrons and ions in a wide energy range. Indeed, wave-particle interaction is a key physics element in the inner magnetospheric dynamics. Thus, understanding the relevant waves is critical and has long been a subject of intense research in space physics.

Whistler chorus waves are usually identified outside the plasmasphere. These waves are believed to play a major role in accelerating electrons in the outer radiation belt (Horne & Thorne 2003, Shprits et al. 2009). The chorus waves can also act to scatter and precipitate electrons into the upper atmosphere (Horne & Thorne 2003, Lam et al. 2010). Other waves such as electromagnetic ion cyclotron waves and plasmaspheric hiss waves can also contribute to atmospheric loss of electrons (Summers & Ni 2007, Kim et al. 2011). The electrons can also be lost into the solar wind through magnetopause crossing under a stressed condition of the solar wind (Kim et al. 2008, 2010, Turner et al. 2012, Hwang et al. 2013). Therefore, the net flux observed by a satellite is determined by a delicate balance between the acceleration (source) and loss effects (Reeves et al. 2003).

In this paper, we focus on the whistler chorus waves. Chorus waves are usually observed in two frequency bands, the lower band at $0.1f_{ce} < f < 0.5f_{ce}$ and the upper band at $0.5f_{ce} < f < 0.8f_{ce}$, with a gap at $0.5f_{ce}$, where f_{ce} is the equatorial electron cyclotron frequency (Burtis & Helliwell 1969, Tsurutani & Smith 1977, Hayakawa et al. 19841989, Koon & Roeder 1990, Santolik et al. 2003). Chorus occurs at both nightside and dayside, and both very near the equator and rather away from the equator (Meredith et al. 2003, Li et al. 2010). The late afternoon to early evening sector is the region where chorus is only rarely observed (Meredith et al. 2003, Li et al. 2010). Occurrence of chorus can extend out to

Received Oct 24, 2014 **Revised** Dec 5, 2014 **Accepted** Dec 5, 2014
†Corresponding Author
E-mail: dylee@chungbuk.ac.kr, ORCID: 0000-0001-9994-7277
Tel: +82-43-261-2316, Fax: +82-43-274-2312

L ~ 10 (Li et al. 2010).

Theories suggest that whistler chorus amplification (at least lower band chorus waves) can be excited by cyclotron resonant interaction with an anisotropic distribution of electrons in the energy of a few to tens of keV that are injected from the plasma sheet into the inner magnetosphere (e.g., Nunn 1974, Katoh & Omura 2007, Omura et al., 2008, Li et al. 2010). Testing this theory using observations is not trivial. It requires simultaneous in-situ measurements, at appropriate positions, of whistler waves and electron velocity distribution with accurate angular resolution from which one can calculate phase space density (PSD). Even if such observations are available, still a major difficulty in interpreting the data remains, which is hard to overcome due to the inherent fact that waves propagate after their generation and particles drift after their injection, each in a completely different way. Therefore, it is generally a rather heavy task to fully clarify the relation between wave generation and particle injection observationally. For this paper we attempt to perform only a simple test for or against the possible development of anisotropic PSD of electrons for a large number of chorus events identified by THEMIS spacecraft (Angelopoulos 2008). We largely confirm the suggested theory.

2. DATA AND METHODOLOGY

We first identify chorus events using the filter bank data of Search Coil Magnetometer (SCM) onboard the THEMIS satellites (Roux et al. 2008). Our method to identify chorus is basically the same as in the previous work by Li et al. (2010). Specifically, we use the data at top three frequency ranges (1390-4000 Hz, 320-904 Hz, 80-227 Hz) out of the six bands of the filter bank data (Cully et al. 2008). After checking individual events visually, we decided to exclude events with a level of 5 pT, 1.3 pT, 1.1 pT or less for the three frequency bands, respectively: These are slightly higher values than the known average noise levels (Golden et al. 2012) such that our selection of events is slightly more conservative. We assume that L = 5 is approximately the inner most boundary where the highest frequency band of the filter bank data can cover the typical chorus frequency range $(0.1\text{-}0.8)f_{ce}$. We collect the chorus events when the satellites are located within L = 5 to 10 as long as the satellites are outside the plasmasphere and not inside the magnetosheath. Also, we limit the satellite position to be |magnetic latitude| ≤ 25°.

The anisotropy in PSD, A, is calculated by the following formula (Li et al. 2010).

$$A = \frac{\int_0^{\pi/2} f(E,\alpha_o)\sin^3\alpha_o d\alpha_o}{2\int_0^{\pi/2}(E,\alpha_o)\cos^3\alpha_o\sin\alpha_o d\alpha_o} - 1 \qquad (1)$$

where α_o is the equatorial pitch angle, E is the electron kinetic energy, and f is the electron PSD. The PSD is calculated using the directional fluxes of electrons at the energies of ~1 keV to ~290 keV observed by Electrostatic Analyzer (ESA) and Solid State Telescope (SST) on THEMIS. A = 0 corresponds to an isotropic pitch angle distribution, A > 0 refers to a pitch angle distribution peaking at 90° (for example, a pancake type distribution) and A < 0 represents a pitch angle distribution minimum at 90° corresponding to a butterfly distribution.

Based on the criteria of identification for chorus events above and given the availability of the THEMIS ESA and SST data, we identified a total of 73 events from THEMIS-A satellite in January 2010 through March 2014. Fig. 1 is the equatorial projection of the THEMIS A satellite positions for the 73 identified events. We deliberately avoided searching for events in the afternoon through dusk to early evening sector, 13-21 MLT, where chorus events of meaningful amplitude rarely occur. Other than this, the MLT distribution of the 73 events is not severely biased toward a particular MLT region. Though the error bars of the fit curve are rather large in Fig. 1, a modest trend is suggestive that the nightside events are slightly closer to the Earth than the

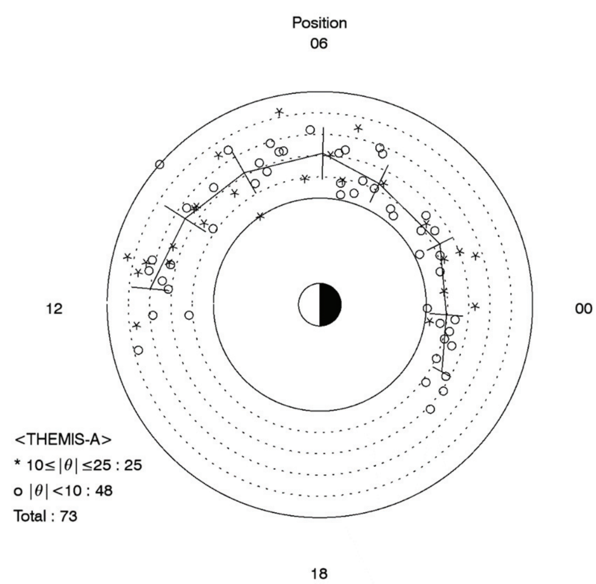

Fig. 1. Equatorial distribution of the THEMIS A positions where 73 chorus events were identified in this work. The inner and outer solid line circles correspond to L = 5 and 10, respectively. Fit curve with an error bar is also shown.

dayside events: This feature of *L*-MLT dependence is well known in the previous studies such as in Li et al. (2010) See Figs. 4-6 in this paper. This spatial dependence is closely related to the resonant condition for chorus excitation which is determined by the ratio of the plasma frequency to the electron cyclotron frequency. Also, Fig. 1 divides the event distribution into two groups according to the magnetic latitude $|\theta| < 10^{o}$ and $10^{o} \leq |\theta| \leq 25^{o}$. The number of events with $|\theta| < 10^{o}$ is about two times larger; this statistics is affected partly by our event selection process.

3. ANALYSIS RESULTS

Fig. 2 shows an example event of chorus activation and associated anisotropy *A* in PSD for two hours interval from 00:44 UT, 14 April 2011. Top panel in Fig. 2 shows the chorus intensity data, and we identify the major chorus intensification at ~01:44 UT when the satellite was at *L* ~ 6.2 near midnight. Earlier than this, around and before 01:14 UT, a number of spikes in the data are present, which we do not identify as a major event. Middle panel in Fig. 2 shows the electron PSD anisotropy *A* in energy-time space. A gradual increase of *A* across the chorus onset time is seen over a certain energy range ~5-15 min prior to the chorus onset. In the other panels, we display the same anisotropy *A* by line plots for each energy channel to help visual inspection. The enhancement in *A* is primarily notable in 1.3 keV, 11.8 keV, and 20.4 keV. For these energies, *A* becomes positive from negative ~5-15 min prior to the chorus onset. The enhancement in *A* is less clear, though still identifiable, at and above 31 keV. Therefore, this is a good example to confirm the possible relation between increased positive anisotropy of electron PSD and chorus enhancement.

Fig. 3 shows another example event of chorus activation and associated anisotropy *A* in PSD on 3 April 2010. From the top panel, we identify two chorus onsets, the first one at ~22:17 UT when the satellite was at *L* ~ 6.2 and MLT ~ 21.6 hr, and the second one at ~22:47 UT, *L* ~ 6.8 and MLT ~ 21.9 hr: See the marks C1 and C2. From the anisotropy panels, we identify the following features. First we discuss the anisotropy features seen closer to the first chorus event C1. For 1.3 keV, *A* greatly increases starting ~35 min before the first chorus onset (A1-a), followed by another rather gradual and weaker increase starting ~7 min before the first chorus onset (A1-b). For 11.8 keV, the situation is similar except that the second increase of *A* (A1-b) is more abrupt and stronger. For 20.4 keV, we see a similar feature as for 11.8 keV, except that the second increase of *A* (A1-b) now begins right at the

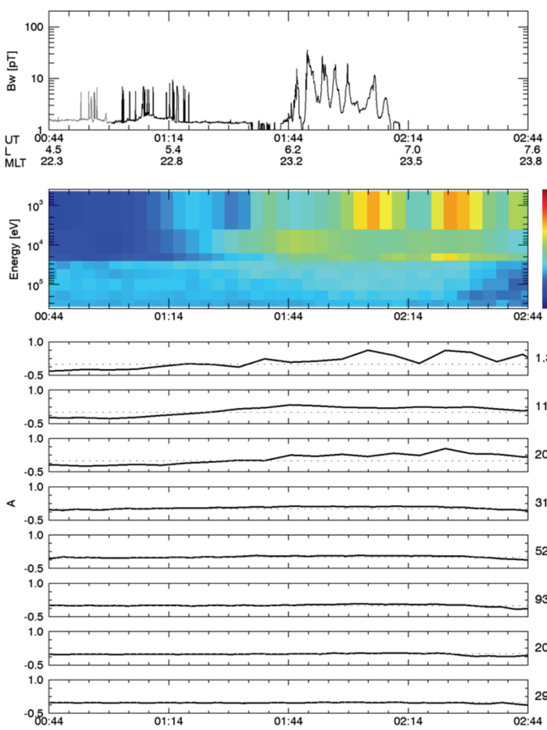

Fig. 2. Chorus event that occurred on 14 April 2011. Top panel shows the chorus intensity, the middle panel shows the gray-scaled anisotropy parameter *A* in energy-time diagram, and the bottom panel is the line plots of the same *A*.

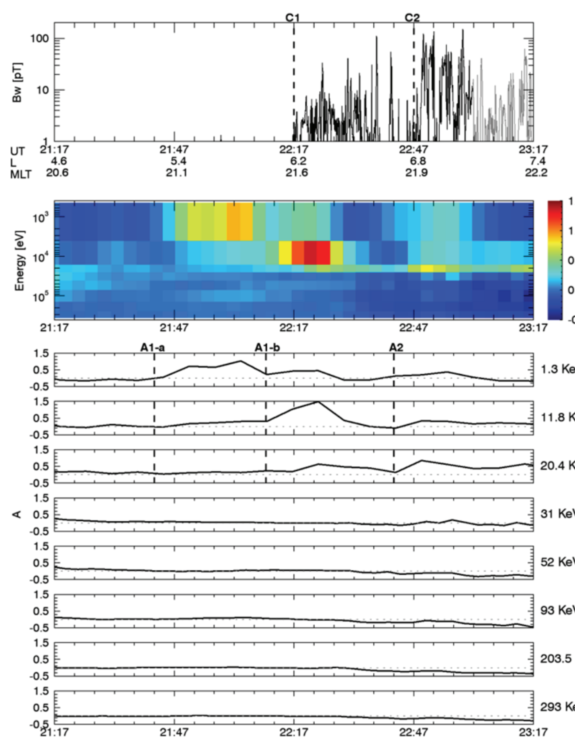

Fig. 3. Same as in Fig. 2 except for the chorus event that occurred on 3 April 2010.

time of the first chorus onset. Indeed, there is a tendency of time delay in onsets of the *A* increases among the energy channels, specifically, between 1.3 keV and 11.8 keV for A1-a and among 1.3, 11.8 and 20 keV for A1-b. On the other hand, the change in *A* is hardly identifiable for 31 keV and higher. In conclusion, we are not sure if and how the earlier anisotropy increase A1-a is related to the first chorus onset C1 but we regard the later anisotropy event A1-b as responsible for the first chorus onset C1. Next we discuss the anisotropy event named A2, seen closer to the second chorus event C2. The increase in *A* is clear at three lowest channels, starting several minutes earlier than the second chorus onset C2. Here again, the major change in *A* is hardly identifiable for 31 keV and higher. Overall, these are all reasonable examples to demonstrate the possible relation between chorus onsets and development of increasing positive anisotropy in electron PSD in the energy range of a few tens of keV or less.

Statistically, after examining PSD for the 73 chorus events, we find that 58 events (~80%) are closely associated with a positive anisotropy *A* which increases around the chorus onsets. Specifically, for these events, we find that *A* becomes above 0.2 from near or below zero within 30 minutes time window prior to chorus onsets (Type 1) or *A* increases at a rate of more than 0.043/min within 30 minutes time window prior to chorus onsets when it is initially well above zero (Type 2). Out of 58 events, 28 and 30 events correspond to Type 1 and 2, respectively: These types are distinguished purely for the sake of convenience with no physical ground. Fig. 4 shows the polar plot of the satellite positions for the 58 events with a fit curve which remains similar to that in Fig. 1. We see no significant bias in the event distribution toward a particular *L*-MLT.

For the 58 events, Fig. 5 shows the number of the events showing an increasing positive *A* at each of the eight energy channels. It indicates that the enhancement in *A* occurs most often at the three lowest channels and rarely at 30 keV and above. We found that for ≥ 30 keV, the enhancement in *A*, when present, is mostly quite weak, and our identification criteria are rather stringent, consequently resulting in the very low number of the event identification for ≥ 30 keV. In addition, we cannot preclude the possibility that this may be partly due to the difference in data quality between two instruments, ESA and SST, on THEMIS since SST covers the energy range of ≥ 30 keV and electron detectors may be sometimes contaminated by protons.

We identify 5 events for which the anisotropy increase occurs in three or more consecutive energy channels with a time delay in increase of *A*: the higher energy is delayed in anisotropy increase relative to the lower energy. Table 1

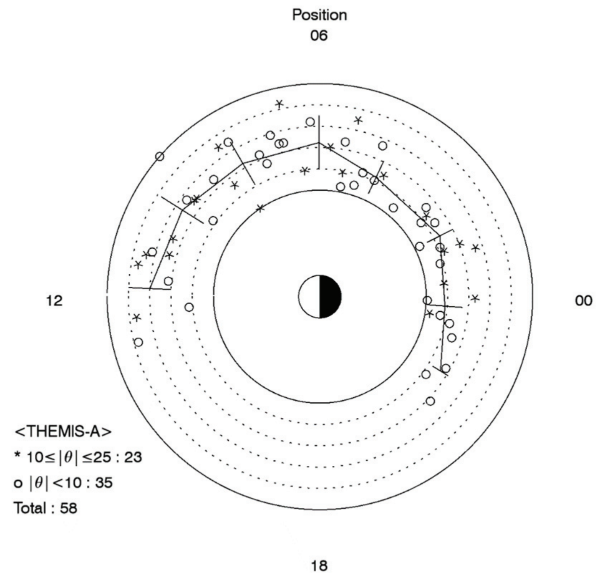

Fig. 4. Equatorial distribution of the THEMIS A positions where 58 chorus events showing increasing anisotropy *A* in electron PSD were identified. Fit curve with an error bar is also shown.

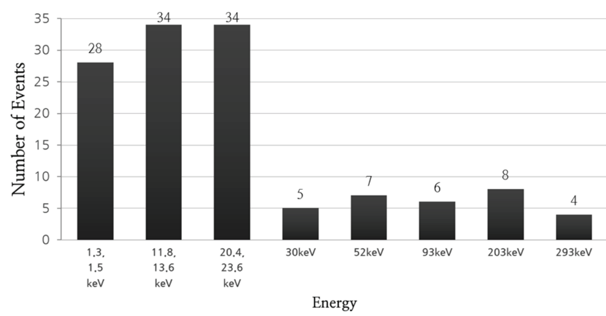

Fig. 5. Number of the events showing increasing and positive anisotropy *A* at each of the 8 energy channels out of the 58 events. For each of the lowest three energies, two energy values are indicated, representing full and reduced mode surveys of the THEMIS ESA instrument, respectively.

shows a summary of the time delay for the 5 events where the delay times are defined by the anisotropy increase time at higher energy relative to that at adjacent lower energy. For example, for the chorus on 2010-03-12 23:51 UT, the anisotropy increase occurs in four consecutive energy channels from 20 keV to 90 keV, and the delay times are 8 min between 20 keV and 30 keV, 3 min between 30 keV and 50 keV, and 1 min between 50 keV and 90 keV. When averaged over all the 5 events, the delay time between two adjacent energies is ~7 min.

Lastly, some previous works suggest that the chorus activation is associated with the substorm onsets which can inject source electrons from the plasma sheet (e.g., Smith et al. 1999). It is reasonable to consider the possibility that the injected electrons can eventually evolve into a PSD state with an enhanced

Table 1. Delay timesa in increase of *A* between the adjacent energies.

Chorus onset	L	MLT	Energy channels [keV]														
			1		10		20		30		50		90		200		290
2010-03-12 23:51 UT	6.5	22.8						8		3		1					
2010-04-01 22:54 UT	6.8	22.0		13		6											
2011-02-12 05:27 UT	5.9	2.4		12		2		20									
2011-02-13 05:48 UT	6.5	2.7		8		5											
2012-04-16 03:45 UT	6.2	1.3		6		0		8									
Number of events				4		4		3		1		1		0		0	
Average delay time [minutes]				9.8		3.3		12.0		3.0		1.0		-		-	

[a] Delay time = Anisotropy onset time of higher energy – that of adjacent lower energy. Given in units of minute.

Table 2. Statistics of *AL* onsets relative to chorus onsets for 24 events.

Time difference bins [minutes]	-60<*t*≤-50	-50<*t*≤-40	-40<*t*≤-30	-30<*t*≤-20	-20<*t*≤-10	-10<*t*≤0
Number of events	1	3	2	6	7	5
Average time difference [minutes]	-56	-56	-34.5	-24	-14.1	-1.8

positive anisotropy, resulting in chorus. We raise the following question whether and how many of our 58 events showing an enhanced positive anisotropy in PSD are well associated, in terms of timing, with substorm onsets. We examine this by checking substorm onsets for the 58 chorus onsets. We determine substorm onsets based on *AL* decrease within the time window of -60 min to 0 relative to chorus onsets. We find that 24 out of the 58 chorus events, ~41 %, are associated with *AL*-decrease onsets within this 60 min time window. Table 2 shows the statistics of the time difference between *AL* onset and chorus onset at each 10 minute-interval bin. The *AL* onset times relative to chorus onsets ranges from within -10 min for five events to -56 min for one event, and the average over all of the events is ~21 min.

4. CONCLUSION AND DISCUSSION

In this work, we examined possible connection of chorus onsets with anisotropy in electron phase space density. This work was based on a number of chorus events and corresponding electron data observed by a THEMIS satellite. Our main goal was to test the statistical significance of the previously suggested scenario that the chorus activation is due to anisotropic electron distribution in a few to tens of keV. Our statistical analysis indicated that this is indeed the case for a majority of the events studied here (~80%), showing positive and increased anisotropy mostly at 20 keV or below. The identified events are overall evenly distributed in MLT between 21 MLT through midnight to 13 MLT.

For some of the studied events, we found an interesting feature that when the increase of the anisotropy occurs at consecutive energy channels, it is earlier by several minutes on average at lower energies than at higher energies. Further study on this feature is worthwhile to pursue in order to understand the cause of this time difference between energies.

We also checked the temporal causality between our chorus events and preceding substorm onsets. We found a rather intermediate percentage rate, ~41 %, for the temporal association of the chorus onsets with preceding substorm onsets. This number may be underestimated. It is because, to check substorm onset, we only looked at the time window of -60 min to 0 min relative to chorus onset, and this may not be sufficient for low energy electrons drifting very slowly around the Earth. Use of a longer time window may be necessary, but then one may begin to feel less confident about the causality between the chorus onset under consideration and a rather remotely identified substorm onset. Despite the limitation of the present analysis, we suspect that substorm injections are only part of the source particles for exciting chorus waves and that other contribution is made by convection from the plasma sheet. Indeed, Lyons et al. (2005) and Hwang et al. (2007) reported periods of enhanced convection when chorus waves were excited. It is well known that convection brings in particles of mainly ~keV or less energy while substorms can inject more energetic particles typically a few tens of keV or higher. Therefore, both should contribute to chorus excitation only at different but partly overlapped energy ranges. In conclusion, we think that positive anisotropy in electron PSD, when increased to a certain level, is the critical factor that determines chorus onsets, no matter what drives the anisotropy by either substorm-injected electrons or convection-driven electrons.

Our work is limited by not distinguishing between the lower and upper band chorus and not seriously examining MLT and latitudinal dependence of anisotropy. Detailed work on these aspects is worthwhile, which we plan to do in near future.

ACKNOWLEDGEMENTS

This work was supported by a research grant of Chungbuk National University in 2013. We acknowledge V. Angelopoulos for use of data from the THEMIS Mission.

REFERENCES

Angelopoulos V, The THEMIS Mission, SSRv 141, 5-34 (2008). http://dx.doi.org/10.1007/s11214-008-9336-1

Burtis WJ, Helliwell RA, Banded chorus: A new type of VLF radiation observed in the magnetosphere by OGO 1 and OGO 3, JGR 74, 3002-3010 (1969). http://dx.doi.org/10.1029/JA074i011p03002

Cully CM, Ergun RE, Stevens K, Nammari A, Westfall J, The THEMIS Digital Fields Board, Space Sci. Rev. 141, 343-355 (2008). http://dx.doi.org/10.1007/s11214-008-9417-1

Golden DI, Spasojevic M, Li W, Nishimura Y, Statistical modeling of in situ hiss amplitudes using ground measurements, JGR 117, A05218 (2012). http://dx.doi.org/10.1029/2011JA017376

Hayakawa M, Muto H, Shimakura S, Hattori K, Parrot M, et al., The wave normal direction of chorus emissions in the outer magnetosphere, Proc. of NIPR SYMP. Upper Atmos. Phys. 2, 62-73 (1989).

Horne RB, Thorne RM, Relativistic electron acceleration and precipitation during resonant interactions with whistler-mode chorus, GRL 30, 1527 (2003). http://dx.doi.org/10.1029/2003GL016973

Hwang JA, Lee DY, Lyons LR, Smith AJ, Zou S, et al., Statistical significance of association between whistler-mode chorus enhancements and enhanced convection periods during high-speed streams, JGR 112, A09213 (2007). http://dx.doi.org/10.1029/2007JA012388

Hwang J, Lee DY, Kim KC, Shin DK, Kim JH, et al., Significant loss of energetic electrons at the heart of the outer radiation belt during weak magnetic storms, JGR 118, 4221-4236 (2013). http://dx.doi.org/10.1002/jgra.50410

Katoh Y, Omura Y, Computer simulation of chorus wave generation in the Earth's inner magnetosphere, GRL 34, L03102 (2007). http://dx.doi.org/10.1029/2006GL028594

Kim KC, Lee DY, Kim HJ, Lyons LR, Lee ES, et al., Numerical calculations of relativistic electron drift loss effect, JGR 113, A09212 (2008). http://dx.doi.org/10.1029/2007JA013011

Kim KC, Lee DY, Kim HJ, Lee ES, Choi CR, Numerical estimates of drift loss and Dst effect for outer radiation belt relativistic electrons with arbitrary pitch angle, JGR 115, A03208 (2010). http://dx.doi.org/10.1029/2009JA014523

Kim KC, Shprits Y, Subbotin D, Ni B, Understanding the dynamic evolution of the relativistic electron slot region including radial and pitch angle diffusion, JGR 116, A10214 (2011). http://dx.doi.org/10.1029/2011JA016684

Koons HC, Roeder JL, A survey of equatorial magnetospheric wave activity between 5 and 8 R_E, Planer. Space Sci., 38 (10), 1335-1341, (1990). http://dx.doi.org/10.1016/0032-0633(90)90136-E

Lam MM, Horne RB, Meredith NP, Glauert SA, Moffat-Griffin T, et al., Origin of energetic electron precipitation > 30 keV into the atmosphere, JGR 115, A00F08 (2010). http://dx.doi.org/10.1029/2009JA014619

Li W, Thorne RM, Nishimura Y, Bortnik J, Angelopoulos V, et al., THEMIS analysis of observed equatorial electron distributions responsible for the chorus excitation, JGR 115, A00F11 (2010). http://dx.doi.org/10.1029/2009JA014845

Li X, Baker DN, O'Brien TP, Xie L, Zong QG, Correlation between the inner edge of outer radiation belt electrons and the inner most plasmapause location, GRL 33, L14107 (2006). http://dx.doi.org/10.1029/2006GL026294

Lyons LR, Lee DY, Thorne RM, Horne RB, Smith AJ, Solar wind-magnetosphere coupling leading to relativistic electron energization during high-speed streams, JGR 110, A11202 (2005). http://dx.doi.org/10.1029/2005JA011254

Meredith NP, Horne RB, Thorne RM, Anderson RR, Favored regions for chorus-driven electron acceleration to relativistic energies in the Earth's outer radiation belt, GRL 30, 1871 (2003). http://dx.doi.org/10.1029/2003GL017698

Nunn D, A self-consistent theory of triggered VLF emissions, P&SS 22, 349-378 (1974). http://dx.doi.org/10.1016/0032-0633(74)90070-1

Omura Y, Katoh Y, Summers D, Theory and simulation of the generation of whistler-mode chorus, JGR 113, A04223, (2008). http://dx.doi.org/10.1029/2007JA012622

Reeves GD, McAdams KL, Friedel RHW, O'Brien TP, Acceleration and loss of relativistic electrons during geomagnetic storms, GRL 30, 1529 (2003). http://dx.doi.org/10.1029/2002GL016513

Roux A, Le Contel O, Coillot C, Bouabdellah A, de la Porte B, et al., The search coil magnetometer for THEMIS, Space Sci. Rev. 141, 265-275 (2008). http://dx.doi.org/10.1007/s11214-008-9455-8

Santolik O, Gurnett DA, Pickett JS, Parrot M, Cornilleau-Wehrlin N, Spatio-temporal structure of storm-time chorus, JGR 108, 1278 (2003). http://dx.doi.org/10.1029/2002JA009791

Shprits YY, Subbotin D, Ni B, Evolution of electron fluxes in the outer radiation belt computed with the VERB code, JGR 114, A11209 (2009). http://dx.doi.org/10.1029/2008JA013784

Smith AJ, Freeman MP, Wickett MG, Cox BD, On the relationship between the magnetic and VLF signatures of the substorm expansion phase, JGR 104, 12351-12360 (1999). http://dx.doi.org/10.1029/1998JA900184

Summers D, Ni B, Meredith NP, Timescales for radiation belt electron acceleration and loss due to resonant wave-particle interactions: 2. Evaluation for VLF chorus, ELF hiss, and electromagnetic ion cyclotron waves, JGR 112, A04207 (2007). http://dx.doi.org/10.1029/2006JA011993

Tsurutani BT, Smith EJ, Two types of magnetospheric ELF chorus and their substorm dependences, JGR 82, 5112-5128 (1977). http://dx.doi.org/10.1029/JA082i032p05112

Turner DL, Shprits Y, Hartinger M, Angelopoulos V, Explaining sudden losses of outer radiation belt electrons during geomagnetic storms, Nature Physics 8, 208-212 (2012). http://dx.doi.org/10.1038/nphys2185